Transient Analysis of a Propagating In-Plane Crack in a Finite Geometry Body Subjected to Static Loadings

Chwan-Huei Tsai[1]
Associate Professor,
Department of Mechanical Engineering,
Huafan College of Humanities
and Technology,
Taipei Hsien, Taiwan 223,
Republic of China

Chien-Ching Ma
Professor,
Department of Mechanical Engineering,
National Taiwan University,
Taipei, Taiwan 10617, Republic of China

In this study, a cracked body with finite boundaries subjected to static loading and the crack propagating with a constant speed are analyzed. The interaction of the propagating crack with reflected waves generated from traction-free boundaries is investigated in detail. The methodology for constructing the scattered field by superimposing the fundamental solution in the Laplace transform domain is proposed. The fundamental solutions represent the responses of applying exponentially distributed loadings in the Laplace transform domain on the surface of a half-plane or a crack. The dynamic stress intensity factors of a propagating crack induced from the interaction with the first few reflected waves generated from the traction-free boundary are obtained in an explicit closed form. The analytical solutions of dynamic stress intensity factors are compared with available numerical and experimental results and the agreement is quite good. We find one thing very interesting: the dynamic stress intensity factor for a long time period is a universal function of the instantaneous extending rate of a crack tip times the static stress intensity factor for an equivalent stationary crack for the finite strip problem. It was also found that the reflected waves generated from free boundaries always increase the stress intensity factor, and the influence from reflected waves generated from the boundary, which is perpendicular to the crack, are weaker than those generated from the boundary, which is parallel to the crack.

1 Introduction

When a static loading is applied to a cracked body and is increased to a sufficiently large magnitude, the crack will begin to extend. The most frequently observed phenomenon in the experiments shows that the crack growth rate is constant during the extending history except in the final unstable or arresting stage. The crack propagating velocity measured experimentally by Kalthoff, Beinert, and Winkler (1977) shows that the assumption of a constant extending rate is acceptable. If the extending rate is high, the inertial effect must be taken into consideration in the analysis. The inherent time dependence of a crack propagation process makes the mathematical models more complex than the equivalent quasi-static models.

The effect of reflected waves interaction with a moving crack had only been discussed in numerical calculation and experimental observations. Kobayashi and Wade (1972) studied the problem of crack propagation and arrest in a tensile plate made of Homalite-100 by using the dynamic photoelastic method. The significant influence of the reflected stress waves generated from the plate boundary was investigated. Experimental results indicated that the reflected waves dominate the stability of crack propagation. The possibility of crack arrest, acceleration, or branching depends on the responses of reflected waves generated from the specimen boundary. Some significant numerical results were obtained by using the finite element method (see Kishimoto, Aoki, and Sakata, 1980). At the same time, Nishioka and Atluri (1980a, b) developed a moving singular element of the finite element method to calculate the dynamic stress intensity factor.

The theoretical analysis of crack propagation, due to general static loading in an unbounded medium, was first addressed by Freund (1972a, b). Freund proposed a superposition method in the time domain to study the dynamic effect of crack propagation in which a fundamental solution is proposed and is used to develop the solution for the negation of the stress distribution on the prospective fracture plane. But this method is valid only for the semi-infinite crack embedded in an infinite medium. Analytical solution for a crack in a finite geometry body is rare. The only available results are provided by Nilsson (1973) and Ma and Ing (1995) for a mode III crack propagating in a finite strip and subjected to static and dynamic loading, respectively.

An interesting conclusion obtained in Freund's paper (1972b) is that the dynamic stress intensity factor has the form of a universal function of an instantaneous extending rate of a crack tip multiplied by the stress intensity factor of an equivalent stationary crack for the unbounded medium problem. The equivalent stationary crack is subjected to the same static loadings and the crack length is equal to the instantaneous length of the actual crack. Whether the above-mentioned result can be generalized in the case of finite boundaries and how the dynamic solutions converge to the corresponding static solution will be discussed in this paper.

A powerful and efficient methodology for constructing the scattered field by superimposing the fundamental solution in the Laplace transform domain has been proposed in recent years by the authors. The Cagniard's method for Laplace inversion is used to obtain the transient solution in a time domain. This methodology was first addressed by Tsai and Ma (1991, 1992)

[1] To whom all correspondence should be addressed.

Contributed by the Applied Mechanics Division of THE AMERICAN SOCIETY OF MECHANICAL ENGINEERS for publication in the ASME JOURNAL OF APPLIED MECHANICS.

Discussion on this paper should be addressed to the Technical Editor, Professor Lewis T. Wheeler, Department of Mechanical Engineering, University of Houston, Houston, TX 77204-4792, and will be accepted until four months after final publication of the paper itself in the ASME JOURNAL OF APPLIED MECHANICS.

Manuscript received by the ASME Applied Mechanics Division, Feb. 14, 1996; final revision, Nov. 20, 1996. Associate Technical Editor: J. W. Ju.

in solving the problems of applying a buried dynamic point body force in a half-plane and a dynamic point body force interaction with a semi-infinite stationary crack. The solution of applying exponentially distributed traction at the surface of a half-plane or a stationary crack face in the Laplace transform domain is considered as the fundamental solution. The reflected and diffracted fields generated from a half-plane and crack tip can be obtained by superimposing the fundamental solutions.

In this paper, the above-mentioned methodology will be generalized and applied in the research of an extending crack. The transient response for a propagating crack with constant velocity in a finite geometry body is obtained by using the generalized method. The orientations of a crack face considered in this study are parallel or perpendicular to the boundary. The main purpose in solving problems concerned with dynamic crack propagation is to determine the dependence of characterizing parameters of the crack-tip field on the applied loading and on the configuration of the body. Since the stress intensity factor is the key parameter in characterizing dynamic crack growth, we will focus our attention mainly on the determination of the dynamic stress intensity factor.

When the stress intensity factor for a stationary crack subjected to static loading reaches its fracture toughness, the crack starts to extend with constant velocity. The diffracted longitudinal wave (denoted by P) and shear wave (denoted by S) will be emitted from the propagating crack tip. The P wave will be reflected from the traction-free-boundary of a half-plane and will generate reflected longitudinal waves and shear waves, which are denoted as PP and PS waves, respectively. Similarly, the S wave will be reflected from the boundary of a half-plane and generate reflected longitudinal (SP) and shear waves (SS). All these reflected waves will arrive at the moving crack tip at a later time and interact with the moving crack. The diffraction, for the second time, will repeat the forward reflection phenomena. In this study, we will neglect the reflected effect on the crack tip of the second time, the third time, etc., because the first reflected waves are much stronger than the reflected waves of later times.

Finally, the analytical solution of a finite cracked body of a rectangular specimen subjected to static loading is obtained without considering the effect of the reflected waves generated from the boundaries perpendicular to the crack and the diffracted waves generated from the corners of the plate. The experimental results obtained by Kalthoff, Beinert, and Winkler (1977), and Hodulak, Kobayashi, and Emery (1990) are discussed and compared with the analytical prediction in light of the present theoretical analysis.

2 Proposed Fundamental Solutions

The solutions of the problem considered in this study can be determined by superposition of the following problems. Problem A treats a static loading applied to a cracked body in an unbounded medium, at time $t = 0$. The crack starts to grow and a new crack propagates out of the original crack with a constant velocity, which will induce a traction on the plane that will eventually define the traction-free boundary of a half-plane. In problem B, a half-plane is considered in which the boundary is subjected to tractions which are equal and opposite to those on the corresponding planes in problem A. Problem C considers an infinite body containing a propagating crack in which the crack face is subjected to the reflected waves which are generated by the half-plane boundary in problem B. The above-mentioned problems A, B, and C are superimposed to construct the solution for propagating crack interaction with stress waves generated from the boundaries.

From physical consideration, the reflected and diffracted waves are generated to eliminate the stress induced by incident waves on the traction-free boundaries. For most of the dynamic problems the stress induced by incident waves can be represented in an integral form of which the kernel is usually an exponential function in the Laplace transform domain of time, so that the solutions of applying exponentially distributed traction at the boundary (surface of half-plane or crack faces) in the Laplace transform domain are considered as the fundamental solutions. The reflected and diffracted waves can be constructed by superimposing the predetermined fundamental solutions in the Laplace transform domain. Some symbols are defined as follows for convenience in the following derivation:

$$\alpha_\pm = \alpha_\pm(\lambda) = [a \pm \lambda(1 \mp av)]^{1/2},$$

$$\alpha_\pm^0 = \alpha_\pm^0(\lambda) = (a \mp \lambda)^{1/2},$$

$$\alpha = \alpha(\lambda) = \alpha_+(\lambda)\alpha_-(\lambda), \quad \alpha^0 = \alpha^0(\lambda) = \alpha_+^0(\lambda)\alpha_-^0(\lambda),$$

$$\beta_\pm = \beta_\pm(\lambda) = [b \pm \lambda(1 \mp bv)]^{1/2},$$

$$\beta_\pm = \beta_\pm^0(\lambda) = (b \mp \lambda)^{1/2},$$

$$\beta = \beta(\lambda) = \beta_+(\lambda)\beta_-(\lambda), \quad \beta^0 = \beta^0(\lambda) = \beta_+^0(\lambda)\beta_-^0(\lambda),$$

$$R = R(\lambda) = (b^2(1 - \lambda v)^2 - 2\lambda^2)^2 + 4\lambda^2\alpha\beta$$

$$= \kappa(d - \lambda)^2(c_1 - \lambda)(c_2 + \lambda)S_+(\lambda)S_-(\lambda),$$

$$\kappa = 4(1 - a^2v^2)^{1/2}(1 - b^2v^2)^{1/2} - (2 - b^2v^2)^2, \quad d = 1/v,$$

$$a_1 = a/(1 + av), \quad b_1 = b/(1 + bv), \quad c_1 = c/(1 + cv),$$

$$a_2 = a/(1 - av), \quad b_2 = b/(1 - bv), \quad c_2 = c/(1 - cv),$$

$$S_\pm = S_\pm(\lambda)$$

$$= \exp\left(\frac{-1}{\pi}\int_{a_{2,1}}^{b_{2,1}} \tan^{-1}\left[\frac{4\xi^2|\alpha||\beta|}{(b^2(1 \mp \xi v)^2 - 2\xi^2)^2}\right]\frac{d\xi}{\xi \pm \lambda}\right),$$

$$R^0 = R^0(\lambda) = R(\lambda)|_{v=0}, \quad S_\pm^0 = S_\pm^0(\lambda) = S_\pm(\lambda)|_{v=0} \quad (1)$$

where a $(=1/v_l)$, b $(=1/v_s)$, and c $(=1/v_r)$ are the slowness of the longitudinal wave, the shear wave and the Rayleigh wave, respectively. Here v_l, v_s, v_r, and v are the propagating speed of the longitudinal wave, shear wave, Rayleigh wave, and the moving crack tip, respectively.

2.1 Fundamental Solution of a Half-Plane. The solution of applying an exponentially distributed loading in the Laplace transform domain at the surface of a half-plane is denoted as the fundamental solution of a half-plane. Consider a half-plane as shown in Fig. 1. An exponentially distributed normal traction in the Laplace transform domain is applied on the surface of the half-plane. The relation between the fixed and moving coordinates is $x_1 = \xi + vt$. The boundary conditions on the half-plane can be written as

$$\bar{\sigma}_{22}(\xi, 0, p) = e^{p\eta\xi} \quad \text{for} \quad -\infty < \xi < \infty, \quad (2)$$

$$\bar{\sigma}_{12}(\xi, 0, p) = 0 \quad \text{for} \quad -\infty < \xi < \infty, \quad (3)$$

where p is the Laplace transform parameter and is assumed to be real and positive, and η is an arbitrary imaginary number. The overbar symbol is used for denoting the transform on time

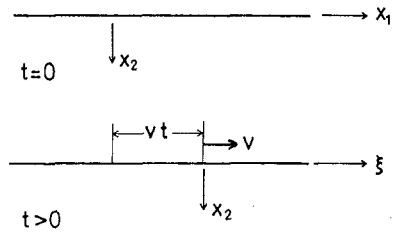

Fig. 1 Configuration and coordinate systems of a half-plane

t. The solutions of stresses that satisfy boundary conditions (2) and (3) can be expressed in the Laplace transform domain as

$$\bar{\sigma}_{11} = \frac{((b^2 - 2a^2)(1 - \eta v)^2 + 2\eta^2)(b^2(1 - \eta v)^2 - 2\eta^2)}{R} \times e^{-p\alpha x_2 + p\eta\xi} + \frac{4\eta^2\alpha\beta}{R} e^{-p\beta x_2 + p\eta\xi}, \quad (4)$$

$$\bar{\sigma}_{12} = \frac{-2\eta\alpha(b^2(1 - \eta v)^2 - 2\eta^2)}{R} e^{-p\alpha x_2 + p\eta\xi} + \frac{2\eta\alpha(b^2(1 - \eta v)^2 - 2\eta^2)}{R} e^{-p\beta x_2 + p\eta\xi}, \quad (5)$$

$$\bar{\sigma}_{22} = \frac{(b^2(1 - \eta v)^2 - 2\eta^2)^2}{R} e^{-p\alpha x_2 + p\eta\xi} + \frac{4\alpha\beta\eta^2}{R} e^{-p\beta x_2 + p\eta\xi}. \quad (6)$$

If the surface traction is applied in the tangential direction, the corresponding boundary conditions are

$$\bar{\sigma}_{22}(\xi, 0, p) = 0 \quad \text{for} \quad -\infty < \xi < \infty, \quad (7)$$

$$\bar{\sigma}_{12}(\xi, 0, p) = e^{p\eta\xi} \quad \text{for} \quad -\infty < \xi < \infty. \quad (8)$$

The solutions of the stresses which satisfy boundary conditions (7) and (8) are expressed in the Laplace transform domain as follows:

$$\bar{\sigma}_{11} = \frac{-2\eta\beta((b^2 - 2a^2)(1 - \eta v)^2 + 2\eta^2)}{R} e^{-p\alpha x_2 + p\eta\xi} + \frac{-2\eta\beta((b^2(1 - \eta v)^2 - 2\eta^2)}{R} e^{-p\beta x_2 + p\eta\xi}, \quad (9)$$

$$\bar{\sigma}_{12} = \frac{4\eta^2\alpha\beta}{R} e^{-p\alpha x_2 + p\eta\xi} + \frac{(b^2(1 - \eta v)^2 - 2\eta^2)^2}{R} e^{-p\beta x_2 + p\eta\xi}, \quad (10)$$

$$\bar{\sigma}_{22} = \frac{-2\eta\beta(b^2(1 - \eta v)^2 - 2\eta^2)}{R} e^{-p\alpha x_2 + p\eta\xi} + \frac{2\eta\beta(b^2(1 - \eta v)^2 - 2\eta^2)}{R} e^{-p\beta x_2 + p\eta\xi}. \quad (11)$$

2.2 Fundamental Solution of a Propagating Crack. The solution of applying an exponentially distributed load in the Laplace transform domain on the propagating crack faces is denoted as the fundamental solution of a propagating crack. Consider a semi-infinite crack propagating with constant speed $v = 1/d$ in an unbounded medium as shown in Fig. 2. The coordinate system (ξ, x_2) is fixed with respect to the moving crack tip and moves with a constant speed v. The upper and lower crack faces are acted by opposite distributed normal tractions which yields the boundary condition in the Laplace transform domain as follows:

$$\bar{\sigma}_{22}(\xi, 0, p) = e^{p\eta\xi} \quad \text{for} \quad -\infty < \xi < 0, \quad (12)$$

$$\bar{\sigma}_{12}(\xi, 0, p) = 0 \quad \text{for} \quad -\infty < \xi < \infty, \quad (13)$$

$$\bar{u}_2(\xi, 0, p) = 0 \quad \text{for} \quad 0 < \xi < \infty, \quad (14)$$

where η is a complex number. Applying the two-sided Laplace transform with respect to ξ and using the Wiener-Hopf technique, the full-field solutions can be obtained as follows:

$$\bar{\sigma}_{ij} = \frac{1}{2\pi i} \int [S^1_{ij}(\lambda) e^{-p\alpha x_2 + p\lambda\xi} + S^2_{ij}(\lambda) e^{-p\beta x_2 + p\lambda\xi}] d\lambda, \quad (15)$$

where

$$S^1_{11}(\lambda) = -((b^2 - 2a^2)(1 - \lambda v)^2 + 2\lambda^2) \times (b^2(1 - \lambda v)^2 - 2\lambda^2)\alpha_+(\eta)G(\eta, \lambda)/\alpha_+(\lambda),$$

$$S^2_{11}(\lambda) = 4\lambda^2\beta(\lambda)\alpha_-(\lambda)\alpha_+(\eta)G(\eta, \lambda),$$

$$S^1_{12}(\lambda) = 2\lambda(b^2(1 - \lambda v)^2 - 2\lambda^2)\alpha_-(\lambda)\alpha_+(\eta)G(\eta, \lambda),$$

$$S^2_{12}(\lambda) = -2\lambda(b^2(1 - \lambda v)^2 - 2\lambda^2)\alpha_-(\lambda)\alpha_+(\eta)G(\eta, \lambda),$$

$$S^1_{22}(\lambda) = -(b^2(1 - \lambda v)^2 - 2\lambda^2)^2\alpha_+(\eta)G(\eta, \lambda)/\alpha_+(\lambda),$$

$$S^2_{22}(\lambda) = -4\lambda^2\beta(\lambda)\alpha_-(\lambda)\alpha_+(\eta)G(\eta, \lambda),$$

$$G(\eta, \lambda) = 1/(\kappa(d - \lambda)^2(c_1 - \lambda) \times (c_2 + \eta)S_-(\lambda)S_+(\eta)(\lambda - \eta)). \quad (16)$$

The associated mode I stress intensity factor expressed in the Laplace transform domain is

$$\bar{K}_I = \frac{-\sqrt{2}}{\sqrt{p}} \frac{\alpha_+(\eta)}{\sqrt{1 - av}\,(c_2 + \eta)S_+(\eta)}. \quad (17)$$

3 Transient Analysis for a Propagating Crack Interaction With Boundaries

Consider a stationary semi-infinite crack subjected to a general static loading, the crack tip is located at $x_1 = 0$ for $t < 0$. Let the resulting normal stress σ_{22} along the crack-tip line $x_1 > 0$, $x_2 = 0$ be $-p(x_1)$, when the loading is increased to a sufficiently large magnitude, the crack will begin to extend at a constant speed and the normal stress $-p(x_1)$ will be released from the growing traction-free surface of the crack along $0 < x_1 < vt$, $x_2 = 0$. The released stress will induce diffracted waves radiating from the moving crack tip. According to the result provided by Freund (1972a), the radiated stress fields σ^*_{ij} and the correspondence stress intensity factor K^*_I can be obtained from the following superposition integral:

$$\sigma^*_{ij}(\xi, x_2, t) = \int_0^{vt} \sigma_{ij}(\xi - x_0, x_2, t - x_0/v)p(x_0)dx_0, \quad (18)$$

$$K^*_I(t) = \int_0^{vt} K_I(t - x_0/v)p(x_0)dx_0 \quad (19)$$

where $\sigma_{ij}(\xi - x_0, x_2, t - x_0/v)$ and $K_I(t - x_0/v)$ are the transient solutions of a crack extending at a constant rate v and subjected to the dynamic concentrated forces of unit magnitude appearing at the crack tip at time $t = x_0/v$.

The diffracted waves emitted from the moving crack tip will be reflected from the boundaries of the finite cracked body. In order to extend Freund's method to apply in the analysis of a finite cracked body, the preliminarily required solutions $\sigma_{ij}(\xi - x_0, x_2, t - x_0/v)$ and $K_I(t - x_0/v)$ with the reflected effect are derived in detail in the following Sections 3.1 to 3.3. Then the stress intensity factor of a crack

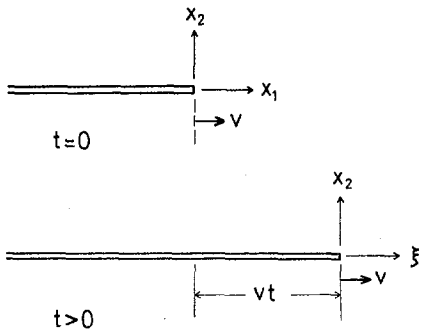

Fig. 2 Configuration and coordinate systems of a propagating crack

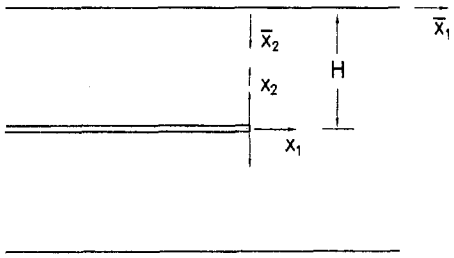

Fig. 3 Configuration and coordinate systems of a semi-infinite crack embedded in a strip

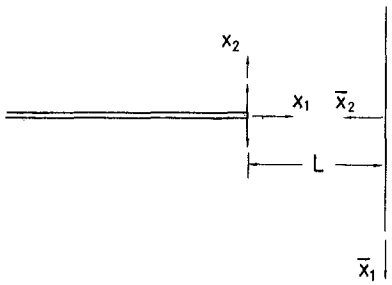

Fig. 4 Configuration and coordinate systems of a semi-infinite crack embedded in a half-plane

in the finite body subjected to a general static loading and extending at a constant speed can be obtained by the superposition integral (19).

3.1 Diffracted Waves in Infinite Medium. A semi-infinite crack moving in a strip and moving in a half-plane is considered in Fig. 3 and Fig. 4, respectively. The distance from the crack tip to the boundary parallel to the crack is denoted as H and to the boundary perpendicular to the crack is denoted as L. The coordinate system (ξ, x_2) is attached at the moving crack tip and the extending rate is v. A concentrated force of unit magnitude is applied at the crack tip at time $t = 0$. Before the diffracted wave generated from the moving crack tip reaches the boundary, the problem can be considered as a semi-infinite crack propagating in an unbounded medium and the boundary conditions can be expressed as follows:

$$\sigma_{22}(\xi, 0, t) = -\delta(\xi + vt)H(t) \quad \text{for} \quad -\infty < \xi < 0, \tag{20}$$

$$\sigma_{12}(\xi, 0, t) = 0 \quad \text{for} \quad -\infty < \xi < \infty, \tag{21}$$

$$u_2(\xi, 0, t) = 0 \quad \text{for} \quad 0 < \xi < \infty. \tag{22}$$

The boundary conditions represented in the Laplace transform domain are

$$\bar{\sigma}_{22}(\xi, 0, t) = -de^{pd\xi} \quad \text{for} \quad -\infty < \xi < 0, \tag{23}$$

$$\bar{\sigma}_{12}(\xi, 0, p) = 0 \quad \text{for} \quad -\infty < \xi < \infty, \tag{24}$$

$$\bar{u}_2(\xi, 0, p) = 0 \quad \text{for} \quad 0 < \xi < \infty. \tag{25}$$

The fundamental solutions for applying the exponentially distributed traction $\bar{\sigma}_{22}(\xi, o, p) = e^{p\eta\xi}$ at crack faces have been obtained in Section 2, so that the radiated diffracted stress fields from the moving crack tip can be obtained by taking $\eta = d$ and multiplying the magnitude $-d$ to (15). The stresses expressed in the Laplace transform domain are

$$\bar{\sigma}_{11}^D = \frac{1}{2\pi i}\int \frac{((b^2 - 2a^2)(1 - \lambda v)^2 + 2\lambda^2)(b^2(1 - \lambda v)^2 - 2\lambda^2)^2)}{\kappa d^2 \alpha_+ (1 - \lambda v)^2 (c_1 - \lambda) S_-(\lambda)} F(\lambda) e^{-p\alpha x_2 + p\lambda\xi}$$
$$- \frac{4\lambda^2 \alpha_- \beta}{\kappa d^2 (1 - \lambda v)^2 (c_1 - \lambda) S_-(\lambda)} F(\lambda) e^{-p\beta x_2 + p\lambda\xi} d\lambda, \tag{26}$$

$$\bar{\sigma}_{22}^D = \frac{1}{2\pi i}\int \frac{(b^2(1 - \lambda v)^2 - 2\lambda^2)^2}{\kappa d^2 \alpha_+ (1 - \lambda v)^2 (c_1 - \lambda) S_-(\lambda)} F(\lambda) e^{-p\alpha x_2 + p\lambda\xi}$$
$$+ \frac{4\lambda^2 \alpha_- \beta}{\kappa d^2 (1 - \lambda v)^2 (c_1 - \lambda) S_-(\lambda)} F(\lambda) e^{-p\beta x_2 + p\lambda\xi} d\lambda, \tag{27}$$

$$\bar{\sigma}_{12}^D = \frac{1}{2\pi i}\int \frac{-2\lambda\alpha_-(b^2(1 - \lambda v)^2 - 2\lambda^2)}{\kappa d^2 (1 - \lambda v)^2 (c_1 - \lambda) S_-(\lambda)} F(\lambda) e^{-p\alpha x_2 + p\lambda\xi}$$
$$+ \frac{2\lambda\alpha_-(b^2(1 - \lambda v)^2 - 2\lambda^2)}{\kappa d^2 (1 - \lambda v)^2 (c_1 - \lambda) S_-(\lambda)} F(\lambda) e^{-p\beta x_2 + p\lambda\xi} d\lambda, \tag{28}$$

where

$$F(\lambda) = \frac{d\alpha_+(d)}{(d - \lambda)(c_2 + d) S_+(d)}. \tag{29}$$

The associated stress intensity factor expressed in the Laplace transform domain can also be obtained by taking $\eta = d$ and multiplying $-d$ to (17) as follows:

$$\bar{K}_I = \frac{d\sqrt{2}\alpha_+(d)}{\sqrt{p}\sqrt{1 - av}(c_2 + d) S_+(d)}. \tag{30}$$

The stress intensity factor in the time domain is

$$K_I = \sqrt{\frac{2}{\pi v t}}\,\kappa(d), \tag{31}$$

where

$$\kappa(d) = \frac{d}{\sqrt{1 - a/d}(c_2 + d) S_+(d)}.$$

3.2 Dynamic Stress Intensity Factors due to Reflected Waves Generated From the Boundary Parallel to the Crack. The diffracted waves emitted from the propagating crack tip will be reflected from the boundary which is parallel to the crack at $x_2 = H$. From Eqs. (27) and (28), it is obvious that the traction, which must be applied at $x_2 = H$ to eliminate the stresses $\bar{\sigma}_{22}^D$ and $\bar{\sigma}_{12}^D$ induced at the boundary, can be represented by the exponential function $e^{p\lambda\xi}$. The fundamental solutions for applying the normal traction $e^{p\eta\xi}$ and tangential traction $e^{p\eta\xi}$ at the surface of the half-plane have already been obtained in (6) and (11).

The reflected waves generated from the boundary can be obtained by superimposing the fundamental solutions as follows:

$$\bar{\sigma}_{22}^{R} = \frac{1}{2\pi i}\int \frac{-(b^2(1-\lambda v)^2-2\lambda^2)^2((b^2(1-\lambda v)^2-2\lambda^2)^2-4\lambda^2\alpha\beta)}{\kappa d^2\alpha_+(1-\lambda v)^2(c_1-\lambda)S_-(\lambda)R}F(\lambda)e^{-pH\alpha-p\alpha\bar{x}_2+p\lambda\xi}d\lambda$$
$$+\frac{1}{2\pi i}\int \frac{-8\lambda^2\alpha_-\beta(b^2(1-\lambda v)^2-2\lambda^2)^2}{\kappa d^2(1-\lambda v)^2(c_1-\lambda)S_-(\lambda)R}F(\lambda)e^{-p\alpha H-p\beta\bar{x}_2+p\lambda\xi}d\lambda$$
$$+\frac{1}{2\pi i}\int \frac{-8\lambda^2\alpha_-\beta(b^2(1-\lambda v)^2-2\lambda^2)^2}{\kappa d^2(1-\lambda v)^2(c_1-\lambda)S_-(\lambda)R}F(\lambda)e^{-p\beta H-p\alpha\bar{x}_2+p\lambda\xi}d\lambda,$$
$$+\frac{1}{2\pi i}\int \frac{4\lambda^2\alpha_-\beta((b^2(1-\lambda v)^2-2\lambda^2)^2-4\lambda^2\alpha\beta)}{\kappa d^2(1-\lambda v)^2(c_1-\lambda)S_-(\lambda)R}F(\lambda)e^{-p\beta H-p\beta\bar{x}_2+p\lambda\xi}d\lambda. \quad (32)$$

It is noted that the traction, which should be applied at $\bar{x}_2 = H$ to eliminate the stress $\bar{\sigma}_{22}^{R}$ at the propagating crack face, is represented by the function $e^{p\lambda\xi}$. The fundamental solution for applying the normal traction $e^{p\eta\xi}$ at the crack surfaces has been expressed in (17), so that the stress intensity factor induced by the reflected waves generated from the boundary can be obtained by superimposing the fundamental solution as follows:

$$\bar{K}_I = \frac{1}{2\pi i p^{1/2}}\int \frac{-2(b^2(1-\lambda v)^2-2\lambda^2)^2((b^2(1-\lambda v)^2-2\lambda^2)^2-4\alpha\beta\lambda^2)}{\sqrt{1-av}\,R^2}F(\lambda)e^{-2p\alpha H}d\lambda$$
$$+\frac{1}{2\pi i p^{1/2}}\int \frac{-32\lambda^2\alpha\beta(b^2(1-\lambda v)^2-2\lambda^2)^2}{\sqrt{1-av}\,R^2}F(\lambda)e^{-p\alpha H-p\beta H}d\lambda$$
$$+\frac{1}{2\pi i p^{1/2}}\int \frac{8\alpha\beta\lambda^2((b^2(1-\lambda v)^2-2\lambda^2)^2-4\alpha\beta\lambda^2)}{\sqrt{1-av}\,R^2}F(\lambda)e^{-2p\beta H}d\lambda. \quad (33)$$

By using the Cagniard-de Hoop method for Laplace inversion, the stress intensity factors in time domain can be obtained, and the results are

$$K_I = \frac{1}{\pi^{3/2}}\int_{T_{PP}}^{t}\frac{1}{\sqrt{t-\tau}}\,\mathrm{Im}\left[\frac{-(b^2(1-\lambda_1 v)^2-2\lambda_1^2)^2((b^2(1-\lambda_1 v)^2-2\lambda_1^2)^2-4\alpha\beta\lambda_1^2)F(\lambda_1)}{\sqrt{1-av}\,R^2}\frac{\partial\lambda_1}{\partial\tau}\right]d\tau$$
$$+\frac{1}{\pi^{3/2}}\int_{T_{PS}}^{t}\frac{1}{\sqrt{t-\tau}}\,\mathrm{Im}\left[\frac{-16\lambda_2^2\alpha\beta(b^2(1-\lambda_2 v)^2-2\lambda_2^2)^2F(\lambda_2)}{\sqrt{1-av}\,R^2}\frac{\partial\lambda_2}{\partial\tau}\right]d\tau$$
$$+\frac{1}{2\pi^{3/2}}\int_{T_{SS}}^{t}\frac{1}{\sqrt{t-\tau}}\,\mathrm{Im}\left[\frac{4\alpha\beta\lambda_3^2((b^2(1-\lambda_3 v)^2-2\lambda_3^2)^2-4\alpha\beta\lambda_3^2)F(\lambda_3)}{\sqrt{1-av}\,R^2}\frac{\partial\lambda_3}{\partial\tau}\right]d\tau, \quad (34)$$

where

$$\lambda_1 = \frac{-2va^2H + i\sqrt{\tau^2 - a^2v^2\tau^2 - 4a^2H^2}}{2H(1-a^2v^2)},$$
$$\lambda_3 = \frac{-2vb^2H + i\sqrt{\tau^2 - b^2v^2\tau^2 - 4b^2H^2}}{2H(1-b^2v^2)},$$

and λ_2 is the root of $\alpha(\lambda)H + \beta(\lambda)H - \tau = 0$. The arrival times are $T_{PP} = 2\sqrt{a_1a_2}\,H$, $T_{SS} = 2\sqrt{b_1b_2}\,H$, $T_{PS} = T_{SP}$, where T_{PS} is the corresponding value of τ at which the imaginary part of λ_2 begins to vanish.

3.3 Dynamic Stress Intensity Factors due to Reflected Waves Generated From the Boundary Perpendicular to the Crack. Now, we consider the case that a propagating crack interaction with the boundary which is perpendicular to the crack as shown in Fig. 4. The diffracted waves expressed by the moving coordinate system (ξ, x_2) can be rewritten in the stationary coordinate system (x_1, x_2) in Laplace transform domain as

$$\bar{\sigma}_{11}^{D} = \frac{1}{2\pi i}\int \frac{((b^2-2a^2)(1-\bar{\lambda}v)^2+2\bar{\lambda}^2)(b^2(1-\bar{\lambda}v)^2-2\bar{\lambda}^2)}{\alpha_+(\bar{\lambda})\kappa d^2(1-\bar{\lambda}v)^2(c_1-\bar{\lambda})S^*(\bar{\lambda})(1+\lambda v)}$$
$$\times F(\bar{\lambda})e^{-p\alpha^0|x_2|+p\lambda x_1}$$
$$-\frac{4\bar{\lambda}^2\alpha_-(\bar{\lambda})\beta(\bar{\lambda})}{\kappa d^2(1-\bar{\lambda}v)^2(c_1-\bar{\lambda})^2(c_1-\bar{\lambda})S_-(\bar{\lambda})(1+\lambda v)}$$
$$\times F(\bar{\lambda})e^{-p\beta^0|x_2|+p\lambda x_1}d\lambda, \quad (35)$$

$$\bar{\sigma}_{12}^{D} = \frac{\mathrm{sgn}\,(x_2)}{2\pi i}\int \frac{-2\bar{\lambda}\alpha_-(\bar{\lambda})(b^2(1-\bar{\lambda}v)^2)-2\bar{\lambda}^2)}{\kappa d^2(1-\bar{\lambda}v)^2(c_1-\bar{\lambda})S_-(\bar{\lambda})(1+\lambda v)}$$
$$\times F(\bar{\lambda})e^{-p\alpha^0|x_2|+p\lambda x_1}$$
$$+\frac{2\bar{\lambda}\alpha_-(\bar{\lambda})(b^2(1-\bar{\lambda}v)^2-2\bar{\lambda}^2)}{\kappa d^2(1-\bar{\lambda}v)^2(c_1-\bar{\lambda})S_-(\bar{\lambda})(1+\lambda v)}$$
$$\times F(\bar{\lambda})e^{-p\beta^0|x_2|+p\lambda x_1}d\lambda, \quad (36)$$

where

$$\bar{\lambda} = \frac{\lambda}{1+\lambda v},$$

and $\mathrm{sgn}\,(x_2) = 1$ for $x_2 > 0$, $\mathrm{sgn}\,(x_2) = -1$ for $x_2 < 0$. The diffracted waves emitted from the crack tip will be reflected from the boundary at some later time. It is obvious to see that the traction, which must be applied at $x_1 = L$ to eliminate the stress $\bar{\sigma}_{11}^{D}$ and $\bar{\sigma}_{12}^{D}$, can be represented by the exponential function $e^{-p\alpha^0|x_2|}$, $e^{-p\beta^0|x_2|}$. The fundamental solutions for applying

normal traction and tangential traction $e^{-p\alpha^0|x_2|}$ or $e^{-p\beta^0|x_2|}$ at the surface of a half-plane were proposed by Tsai and Ma (1991). So that the reflected waves can be obtained by superimposing the fundamental solutions as follows:

and

$$\tilde{\alpha} = \alpha(\tilde{\lambda}), \quad \bar{\alpha} = \alpha(\bar{\lambda}), \quad \bar{\alpha}^0 = \alpha^0(\bar{\lambda}),$$
$$\tilde{\beta} = \beta(\tilde{\lambda}), \quad \bar{\beta} = \beta(\bar{\lambda}), \quad \bar{\beta}^0 = \beta^0(\bar{\lambda}),$$

$$\bar{\sigma}_{22}^R = \frac{1}{2\pi i}\int \left[\frac{-((b^2-2a^2)(1-\bar{\lambda}v)^2+2\bar{\lambda}^2)(b^2(1-\bar{\lambda}v)^2-2\bar{\lambda}^2)(b^2-2\alpha^{02})(b^2-2\lambda^2)F(\bar{\lambda})}{\alpha_+(\bar{\lambda})\kappa d^2(1-\bar{\lambda}v)^2(c_1-\bar{\lambda})S_-(\bar{\lambda})(1-\lambda v)R^0(\alpha^0)}\right.$$
$$\left. - \frac{4g\bar{\lambda}(b^2(1-\bar{\lambda}v)^2-2\bar{\lambda}^2)\alpha_-(\bar{\lambda})\alpha^0\beta^0(\alpha^0)(b^2-2\lambda^2)F(\bar{\lambda})}{\kappa d^2(1-\bar{\lambda}v)^2(c_1-\bar{\lambda})S_-(\bar{\lambda})(1-\lambda v)R^0(\alpha^0)}\right] e^{-2p\lambda L+p\lambda x_1} d\lambda$$
$$+ \frac{1}{2\pi i}\int \frac{8((b^2-2a^2)(1-\bar{\lambda}v)^2+2\bar{\lambda}^2)(b^2(1-\bar{\lambda}v)^2-2\lambda^2)\alpha_-(\bar{\lambda})\lambda^2\beta^{02}F(\bar{\lambda})}{\alpha_+(\bar{\lambda})\kappa d^2(1-\bar{\lambda}v)^2(c_1-\bar{\lambda})S_-(\bar{\lambda})(1-\alpha^0(\beta^0)v)R^0(\beta^0)} e^{-p\alpha^0(\beta^0)L-p\lambda L+p\lambda x_1} d\lambda$$
$$+ \frac{1}{2\pi i}\int \frac{-8\bar{\lambda}^2\beta(\bar{\lambda})\alpha_-(\bar{\lambda})(b^2-2\beta^0(\alpha^0)^2)(b^2-2\lambda^2)\lambda F(\bar{\lambda})}{\kappa d^2(1-\bar{\lambda}v)^2(c_1-\bar{\lambda})S_-(\bar{\lambda})(1-\beta^0(\alpha^0)v)R^0(\bar{\alpha}^0)} e^{-p\beta^0(\alpha^0)L-p\lambda L+p\lambda x_1} d\lambda$$
$$+ \frac{1}{2\pi i}\int \frac{-16\bar{\lambda}^2\beta(\bar{\lambda})\alpha_-(\bar{\lambda})\lambda\beta^{02}\alpha^0(\beta^0) - 4\bar{\lambda}\lambda(b^2(1-\bar{\lambda}v)^2-2\bar{\lambda}^2)\alpha_-(\bar{\lambda})\beta^0(b^2-2\lambda^2)F(\bar{\lambda})}{\kappa d^2(1-\bar{\lambda}v)^2(c_1-\bar{\lambda})S_-(\bar{\lambda})(1-\lambda v)R^0(\beta^0)} e^{-2p\lambda L+p\lambda x_1} d\lambda \quad (37)$$

where

$$\bar{\lambda} = \frac{-\lambda}{1-\lambda v}$$

for the first and fourth terms, and

$$\bar{\lambda} = \frac{-\alpha^0(\beta^0)}{1-\alpha^0(\beta^0)v}, \quad \bar{\lambda} = \frac{-\beta^0(\alpha^0)}{1-\beta^0(\alpha^0)v}$$

for the second and third terms.

In order to obtain the stress intensity factor attributed to the reflected waves, the reflected waves must be transformed to the moving coordinate system (ξ, x_2) by using the transformation principle. The stress intensity factor induced by reflected waves generated from the boundary can be expressed as follows:

$$\bar{K}_I = \frac{\sqrt{2}}{2\pi i p^{1/2}}\int G_1(\lambda)e^{-2p\lambda L}d\lambda + \frac{\sqrt{2}}{2\pi i p^{1/2}}\int G_2(\lambda)e^{-p\lambda L-p\alpha^0(\bar{\beta}^0)(1-\lambda v)L}d\lambda + \frac{\sqrt{2}}{2\pi i p^{1/2}}\int G_3(\lambda)e^{-p\lambda L-p\beta^0(\bar{\alpha}^0)(1-\lambda v)L}d\lambda + \frac{\sqrt{2}}{2\pi i p^{1/2}}\int G_4(\lambda)e^{-2p\lambda L}d\lambda, \quad (38)$$

where

$$\bar{\lambda} = \frac{\lambda}{1-\lambda v}, \quad F'(\tilde{\lambda}) = \frac{\alpha_+(\lambda)}{\sqrt{1-av}\,(c_2+\lambda)S_+(\lambda)}F(\tilde{\lambda}), \quad (40)$$

and

$$\tilde{\lambda} = \frac{-\lambda}{1-2\lambda v},$$

for the first and fourth terms of (38),

$$\tilde{\lambda} = \frac{-\alpha^0(\bar{\beta}^0)}{1-\alpha^0(\bar{\beta}^0)v}, \quad \tilde{\lambda} = \frac{-\beta^0(\bar{\alpha}^0)}{1-\beta^0(\bar{\alpha}^0)v},$$

for the second and third terms of (38). By using the Cagniard-de Hoop method, the stress intensity factors can be obtained in the time domain as follows:

$$K_I = \frac{1}{\pi^{3/2}}\int_{T_{PP}}^{t}\frac{1}{\sqrt{t-\tau}}\,\mathrm{Im}\left[G_1(\lambda_1)\frac{\partial\lambda_1}{\partial\tau}\right]d\tau + \frac{1}{\pi^{3/2}}\int_{T_{PS}}^{t}\frac{1}{\sqrt{t-\tau}}\,\mathrm{Im}\left[G_2(\lambda_2)\frac{\partial\lambda_2}{\partial\tau}\right]d\tau + \frac{1}{\pi^{3/2}}\int_{T_{SP}}^{t}\frac{1}{\sqrt{t-\tau}}\,\mathrm{Im}\left[G_3(\lambda_3)\frac{\partial\lambda_3}{\partial\tau}\right]d\tau$$

$$G_1(\lambda) = \frac{((b^2-2a^2)(1-\tilde{\lambda}v)^2+2\tilde{\lambda}^2)(b^2(1-\tilde{\lambda}v)^2-2\tilde{\lambda}^2)\tilde{\alpha}_-(b^2-2\bar{\alpha}^{02})(b^2-2\lambda^2)F'(\tilde{\lambda})}{\kappa d^2(1-\tilde{\lambda}v)^2\tilde{\alpha}(c_1-\tilde{\lambda})S_-(\tilde{\lambda})(1-\bar{\lambda}v)(1-\lambda v)R^0(\bar{\alpha}^0)} + \frac{4\tilde{\lambda}(b^2(1-\tilde{\lambda}v)^2-2\tilde{\lambda}^2)\tilde{\alpha}_-\bar{\alpha}^0\beta^0(\bar{\alpha}^0)(b^2-2\bar{\lambda}^2)F'(\tilde{\lambda})}{\kappa d^2(1-\tilde{\lambda}v)^2(c_1-\tilde{\lambda})S_-(\tilde{\lambda})(1-\bar{\lambda}v)(1-\lambda v)R^0(\bar{\alpha}^0)}$$

$$G_2(\lambda) = \frac{-8\bar{\lambda}^2\bar{\beta}^2((b^2-2a^2)(1-\tilde{\lambda}v)^2+2\tilde{\lambda}^2)(b^2(1-\tilde{\lambda}v)^2-2\tilde{\lambda}^2)F'(\tilde{\lambda})}{\kappa d^2(1-\tilde{\lambda}v)^2\tilde{\alpha}_+(c_1-\tilde{\lambda})S_-(\tilde{\lambda})(1-\alpha^0(\bar{\beta}^0)v)R^0(\bar{\beta}^0)(1-\lambda v)}$$

$$G_3(\lambda) = \frac{8\tilde{\lambda}^2\tilde{\beta}\tilde{\alpha}_+(b^2-2\beta^0(\bar{\alpha}^0)^2)(b^2-2\bar{\lambda}^2)\bar{\lambda}F'(\tilde{\lambda})}{\kappa d^2(1-\tilde{\lambda}v)^2(c_1-\tilde{\lambda})S_-(\tilde{\lambda})(1-\beta^0(\bar{\alpha}^0)v)R^0(\bar{\alpha}^0)(1-\lambda v)}$$

$$G_4(\lambda) = \frac{16\tilde{\lambda}^2\tilde{\beta}\tilde{\alpha}_-\bar{\beta}^{02}\alpha^0(\bar{\beta}^0)\bar{\lambda} + 4\tilde{\lambda}(b^2(1-\tilde{\lambda}v)^2-2\tilde{\lambda}^2)\tilde{\alpha}_-\bar{\lambda}\bar{\beta}^0(b^2-2\bar{\lambda}^2)F'(\tilde{\lambda})}{\kappa d^2(1-\tilde{\lambda}v)^2(c_1-\tilde{\lambda})S_-(\tilde{\lambda})(1-\bar{\lambda}v)(1-\lambda v)R^0(\bar{\beta}^0)}, \quad (39)$$

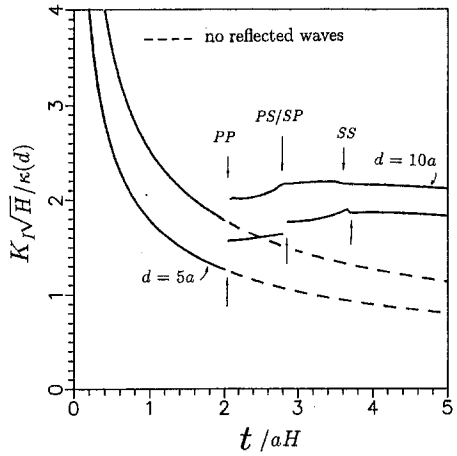

Fig. 5 Stress intensity factors of an embedded crack in a strip subjected to a pair of concentrated forces applied at $x_1 = 0$

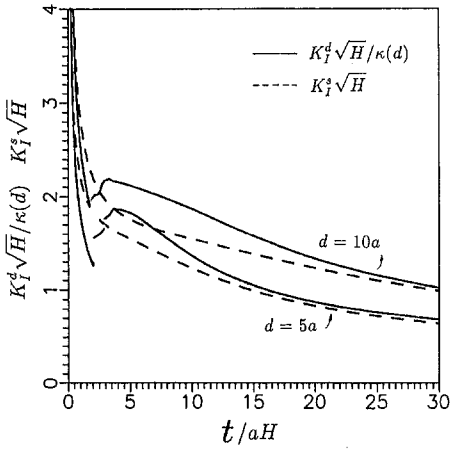

Fig. 6 Dynamic and static stress intensity factors (K_I^d, K_I^s) of a crack embedded in a strip subjected to a pair of concentrated forces applied at $x_1 = 0$

$$+\frac{1}{\pi^{3/2}}\int_{T_{SS}}^{t}\frac{1}{\sqrt{t-\tau}}\,\mathrm{Im}\left[G_4(\lambda_4)\frac{\partial\lambda_4}{\partial\tau}\right]d\tau, \quad (41)$$

where $\lambda_1 = \lambda_4 = (\tau/2L)$ and λ_2 and λ_3 are the roots of

$$\lambda L + \alpha^0(\bar{\beta}^0)(1 - \lambda v)L - \tau = 0,$$

and

$$\lambda L + \beta^0(\bar{\alpha}^0)(1 - \lambda v)L - \tau = 0,$$

respectively. The correspondent arrival times are

$$T_{PP} = 2a_1L, \quad T_{PS} = \frac{aL}{1+bv} + b_1L,$$

$$T_{SP} = \frac{bL}{1+av} + a_1L, \quad T_{SS} = 2b_1L. \quad (42)$$

4 Numerical Results

With the analytic solution constructed in the previous section, we now perform the numerical investigation of the dynamic stress intensity factor for a propagating crack interaction with stress waves reflected from boundaries. In this study, Poisson's ratio ν is assumed to be equal to 0.25 which gives ratios of the slowness of $b = \sqrt{3}\,a$ and $c = 1.884a$. First, the results of an embedded semi-infinite crack contained in a finite strip and in a half-plane, as shown in Figs. 3 and 4, are investigated. At time $t = 0$, a concentrated force of unit magnitude is applied at the crack tip, and the crack begins to propagate along the crack tip line with constant speed v. The extending rates $v = 0.1v_l$, $0.2v_l$ (i.e., slowness ratios $d/a = 10, 5$) are chosen for numerical investigation.

For the case of a semi-infinite crack which is embedded parallel to the boundaries of the strip (i.e. Fig. 3), the diffracted waves will be emitted from the propagating crack tip and will be reflected from the two boundaries of the strip. The transient results for the dynamic stress intensity factors are shown in Fig. 5. At the time $t = 2.04aH$ ($=2.01aH$), the reflected PP wave for the extending slownesses $d/a = 5$ ($=10$) arrives at the propagating crack tip. The reflected waves from the boundaries will enlarge the stress intensity factor. The dash line represents the stress intensity factor without considering the reflected waves from the boundaries, i.e., a semi-infinite crack propagates in an unbounded medium.

In order to understand how dynamic transient response approaches the corresponding static value the long-time behavior, which accounts only the first few reflected waves, is calculated and shown in Fig. 6. The dynamic stress intensity factors K_I^d divided by the universal function $\kappa(d)$ are presented by solid lines that are evaluated without considering the reflected waves of the second time, the third time, etc., from the horizontal boundary. The dash lines represent the equivalent static solution K_I^s at which the point loading is applied at a distance vt from the crack tip. It is shown that these two lines will approach each other as time is large. Even though the reflected waves of the second time, the third time, etc, are neglected in the numerical calculation, it is reasonable to concluded that the long-time behavior of a stress intensity factor of a propagating crack in a strip has the form of a universal function $\kappa(d)$ of an instantaneous extending rate of crack tip multiplied by the stress intensity factor for a stationary crack with the instantaneous length of the actual crack subjected to the same static loadings. Hence, Freund's result (1972b) is shown to be valid for the finite strip problem also. It is also concluded that the result is accurate enough to evaluate the dynamic stress intensity factor without considering the reflected waves of the second time, the third time, etc., and only when taking the first reflected waves into consideration. The result will cause only a small tolerance (about six percent) in the calculation of dynamic stress intensity factor.

For the case of a semi-infinite crack which is embedded perpendicularly to the boundaries of a half-plane (i.e., Fig. 4), the numerical results of transient stress intensity factors are shown in Fig. 7. The dashed line represents the value without

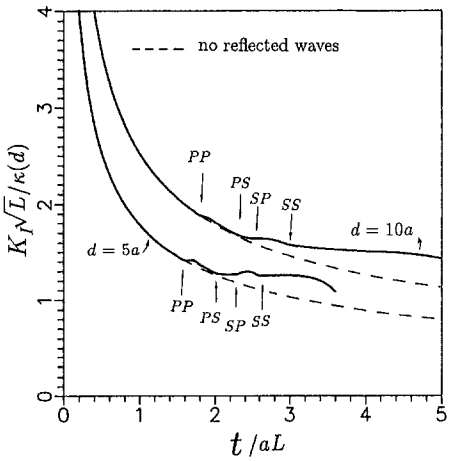

Fig. 7 Stress intensity factors of an embedded crack in a half-plane subjected to a pair of concentrated forces applied at $x_1 = 0$

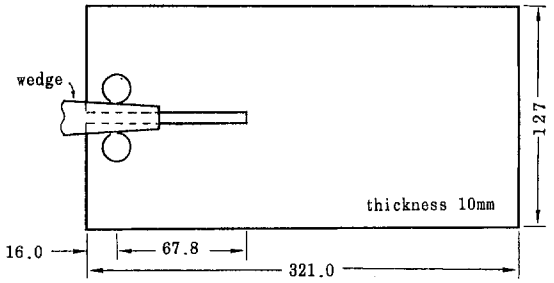

Fig. 8 Specimen configuration of rectangular double cantilever specimen investigated by Kalthoff et al. (1977) and Atluri et al. (1985)

considering the contribution from reflected waves. At time $t = 1.67aL$ ($=1.82aL$), the reflected PP wave generated from the boundary for the extending slownesses $d/a = 5$ ($=10$) arrives at the propagating crack tip. Unlike the case of an embedded crack in a strip as discussed in Fig. 5, the reflected effect for this case is relatively small.

Next, experimental results reported by Kalthoff, Beinert, and Winkler (1977) and the numerical results reported by Atluri and Nishioka (1985) are discussed, and both results will be compared with the present analytical solutions. A rectangular double-cantilever specimen made by photoelastic material Araldite B, as shown in Fig. 8, is considered. The material properties of Araldite B are density $\rho = 1047$ kg/m^3, Poisson's ratio $\nu = 0.33$, Young's modulus $E = 3.38$ GPa, which yield the longitudinal wave speed $v_l = 1903$ m/s, shear wave speed $v_s = 1102$ m/s, and Rayleigh wave speed $v_R = 1081$ m/s. When a static loading is applied and is increased to the the fracture toughness $K_C = 2.32$ MPa $\sqrt{m}$, the crack begins to extend at a constant speed $v = 295$ m/s during the early 300 μs.

The function $p(x_1)$ as shown in (18), which is the resulting negation of the stress σ_{22} ahead of the crack tip before extension occurred, is calculated by the finite element method. Then substitute the numerical result of $p(x_1)$ into (18), the stress intensity factor can be obtained based on the analysis in the previous section and the result is shown in Fig. 9. Since the reflected effect generated from boundaries perpendicular to a crack and reflected waves of the second time, the third time, etc., are small enough, only the first few reflected waves generated from the boundaries parallel to the crack are considered in the analysis. The results based on the theoretical solution are consistent with the finite element results of Atluri and Nishioka (1985) and experimental results of Kalthoff, Beinert, and Winkler (1977).

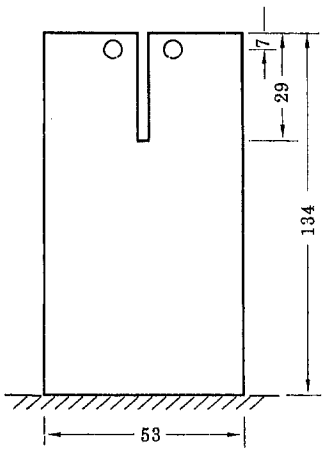

Fig. 10 Specimen configuration of rectangular double cantilever specimen investigated by Hodulak et al. (1980)

The equivalent static stress intensity factor for the given crack growing length referred to in Kalthoff (1985) is also presented in Fig. 9.

At the instant of crack propagation, the stress intensity factor jumps from 2.32 MPa $\sqrt{m}$ to 2.07 MPa $\sqrt{m}$ with the decreasing ratio $\kappa(d)$, where $d = (v_l/v)a = 6.45a$. Because the kinetic energy is radiated into the specimen, the dynamic stress intensity factor is smaller than the equivalent static stress intensity factor for the given crack growing length (i.e., $K_I^d < K_I^s$). As the crack continuously propagates, the distance between the loading point and crack tip will increase, and the stress intensity factor will decrease. After the first reflected PP wave arrives at the crack tip (i.e., at time $t = 67.55$ μs), the tensile effect of the reflected waves will slow down the decay effect of the stress intensity factor and make $K_I^d > K_I^s$.

Finally, a similar photoelastic specimen of material Araldite B, as shown in Fig. 10, which is studied by Hodulak, Kobayashi and Emery (1980), is considered. When the loading is increased up to the the fracture toughness $K_C = 2.0$ MPa $\sqrt{m}$, the crack begins to extend at a constant speed $v = 240$ m/s. By using the same procedure as mentioned in the foregoing problem, the finite element method is applied to obtain the stress distribution function $p(x_1)$ along the crack-tip line, and the dynamic stress intensity factors are shown in Fig. 11. The theoretical results presented in this study are consistent with the finite element results and experimental results by Hodulak, Kobayashi, and

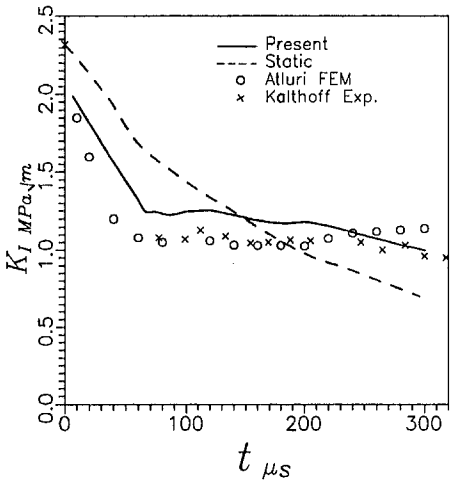

Fig. 9 Dynamic stress intensity factor of a propagating crack as shown in Fig. 8

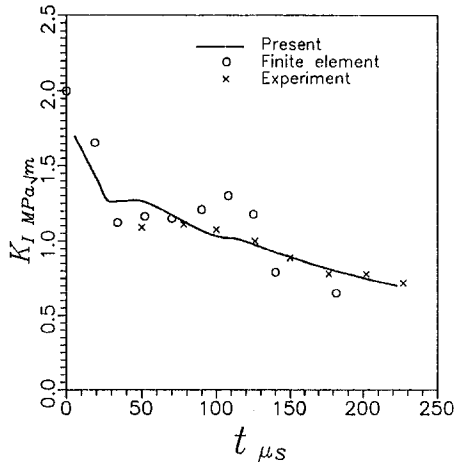

Fig. 11 Dynamic stress intensity factor of a propagating crack as shown in Fig. 10

Emery (1980). At the instant of crack propagation, the stress intensity factor jumps from 2.0 MPa $\sqrt{m}$ to 1.81 MPa $\sqrt{m}$ with the decreasing ratio $\kappa(d)$, where $d = (v_l/v)a = 7.93a$. At time $t = 28.07$ μs, the reflected PP wave returns to the crack tip and induces a tensile effect for the crack which will slow down the decay behavior of the stress intensity factor.

5 Conclusion

A powerful method for the theoretical formulation of a crack propagating in finite boundaries and subjected to general static loading is proposed in this study. The effects of reflected waves generated from boundaries and their interaction with a propagating crack have been successfully obtained and are shown to be in good agreement with the existing experimental and numerical results.

Freund's remarkable result (1972b) for crack propagating in an unbounded medium is shown to be valid for the finite strip problem also. For the finite boundary problem, we have shown that the long-time behavior of the stress intensity factor possesses the form of a universal function $\kappa(d)$ of an instantaneous extending rate of a crack tip multiplied by the stress intensity factor of an equivalent stationary crack. The equivalent stationary crack is subjected to the same static loading and the crack length is equal to the instantaneous length of the actual crack. It is also concluded that the result is accurate enough to evaluate the dynamic stress intensity factor without considering the contribution for reflected waves of the second time, the third time, etc., and only when taking the first reflected waves into consideration, which will result only in a small tolerance (about six percent) in the calculation of the long-time behavior.

The reflected waves generated from the boundary, which is parallel to a crack, have a stronger influence on the stress intensity factor of crack propagation than that generated from the boundary perpendicular to a crack. The reflected waves usually behave as a tensile effect, the dynamic stress intensity factor will generally increase after the reflected waves generated from a free boundary arrive at the crack tip.

There still are many unanswered questions in dynamic fracture and this work may provide a useful technique for further investigation in more complicated dynamic fracture problems, especially on the crack propagation event. The proposed method in this study has already been extended to solve more difficult problems of crack propagation in a finite geometry body subjected to dynamic impact loadings, and the results will be shown in a future paper.

Acknowledgment

The authors gratefully acknowledge the financial support of this research by the National Science Council (Republic of China) under Grant NSC 81-0401-E002-18 to National Taiwan University.

References

Atluri, S. N., and Nishioka, T., 1985, "Numerical Studies in Dynamic Fracture Mechanics," *International Journal of Fracture,* Vol. 27, pp. 245–261.

Freund, L. B., 1972a, "Crack Propagation in an Elastic Solid Subjected to General Loading–I. Constant Rate of Extension," *Journal of the Mechanics and Physics of Solids,* Vol. 20, pp. 129–140.

Freund, L. B., 1972b, "Crack Propagation in an Elastic Solid Subjected to General Loading–II. Non-uniform Rate of Extension," *Journal of the Mechanics and Physics of Solids,* Vol. 20, pp. 141–152.

Hodulak, L., Kobayashi, A. S., and Emery, A. F., 1980, "Influence of Dynamic Fracture Toughness on Dynamic Crack Propagation," *Engineering Fracture Mechanics,* Vol. 13, pp. 85–93.

Kalthoff, J. F., Beinert, J., and Winkler, S., 1977, *Fast Fracture and Crack Arrest,* G. T. Hahn et al., eds., ASTM STP 627 pp. 161–176.

Kalthoff, J. F., 1985, "On the Measurement of Dynamic Fracture Toughnesses," *International Journal of Fracture,* Vol. 27, pp. 277–298.

Kishimoto, S. Aoki, and Sakata M., 1980, "Computer Simulation of Fast Crack Propagation in Brittle Material," *International Journal of Fracture,* Vol. 16, pp. 3–13.

Kobayashi, A. S., and Wade, B. G., 1972, "Crack Propagation and Arrest in Impact Plates," *Proceeding of an International Conference on Dynamic Crack Propagation,* G. C. Sih, ed., Lehigh University, Lehigh, PA, pp. 663–678.

Ma, C. C., and Ing, Y. S., 1995, "Transient Analysis of Dynamic Crack Propagation with Boundary Effect," ASME JOURNAL OF APPLIED MECHANICS, Vol. 62, pp. 1029–1038.

Nilsson, F., 1973, "A Transient Crack Problem for an Infinite Strip under Antiplane Shear," *Dynamic Crack Propagation,* G. C. Sih, ed., Nordhoff, Dordrecht, The Netherlands, pp. 543–551.

Nishioka, T., and Atluri, S. N., 1980, "Numerical Modeling of Dynamic Crack Propagation in Finite Bodies, by Moving Singular Elements Part 1: Formulation," ASME JOURNAL OF APPLIED MECHANICS, Vol. 47, pp. 570–576.

Nishioka, T., and Atluri, S. N., 1980, "Numerical Modeling of Dynamic Crack Propagation in Finite Bodies, by Moving Singular Elements Part 2: Results," ASME JOURNAL OF APPLIED MECHANICS, Vol. 47, pp. 577–582.

Ravi-Chandar, K., and Knauss, W. G., 1982, "Dynamic Crack-tip Stresses Under Stress Wave Loading: A Comparison of Theory and Experiment," *International Journal of Fracture,* Vol. 20, pp. 209–222.

Ravi-Chandar, K., and Knauss, W. G., 1984, "An Experimental Investigation into Dynamic Fracture: II. Microstructural Aspects," *International Journal of Fracture,* Vol. 26, pp. 65–80.

Tsai, C. H., and Ma, C. C., 1991, "Exact Transient Solutions of Buried Dynamic Point Forces and Displacement Jumps for an Elastic Half Space," *International Journal of Solids and Structures,* Vol. 28, pp. 955–974.

Tsai, C. H., and Ma, C. C., 1992, "Transient Analysis of a Semi-infinite Crack Subjected to Dynamic Concentrated Forces," ASME JOURNAL OF APPLIED MECHANICS, Vol. 59, pp. 804–811.